Reconfigurable water-substrate based antennas with temperature control

Ahmed Toaha Mobashsher and Amin Abbosh

Citation: Appl. Phys. Lett. **110**, 253503 (2017); doi: 10.1063/1.4986788
View online: http://dx.doi.org/10.1063/1.4986788
View Table of Contents: http://aip.scitation.org/toc/apl/110/25
Published by the American Institute of Physics

Reconfigurable water-substrate based antennas with temperature control

Ahmed Toaha Mobashsher[a] and Amin Abbosh
School of ITEE, The University of Queensland, St. Lucia, QLD 4072, Australia

(Received 17 March 2017; accepted 6 June 2017; published online 19 June 2017)

We report an unexplored reconfigurable antenna development technique utilizing the concept of temperature variable electromagnetic properties of water. By applying this physical phenomena, we present highly efficient water-substrate based antennas whose operating frequencies can be continuously tuned. While taking the advantage of cost-effectiveness of liquid water, this dynamic tuning technique also alleviates the roadblocks to widespread use of reconfigurable liquid-based antennas for VHF and UHF bands. The dynamic reconfigurability is controlled merely via external thermal stimulus and does not require any physical change of the resonating structure. We demonstrate dynamic control of omnidirectional and directional antennas covering more than 14 and 12% fractional bandwidths accordingly, with more than 85% radiation efficiency. Our temperature control approach paves the intriguing way of exploring dynamic reconfigurability of water-based compact electromagnetic devices for non-static, in-motion and low-cost real-world applications. *Published by AIP Publishing*. [http://dx.doi.org/10.1063/1.4986788]

In recent years, there has been a growing interest in using liquidity of metals and substrates in realizing reconfigurable devices from the microwave to the optical parts of the spectrum. Liquid metals [Eutectic gallium indium (EGaIn),[1,2] Mercury,[3,4] Galinstan,[5] etc.] attain frequency reconfigurable operation by using pressure[6,7] or electrical potential[8,9] variations. Substrates, like liquid crystals,[10] mechanically[11] or thermally[12] controllable dielectric particles, nano-patterned meta-surfaces,[13] meta-liquid crystals,[14] and water[15] are also popularly used for reconfigurable electromagnetic applications. Considering the access, expense, and complexity of operation, water is more attractive when compared to other liquids. However, in most of the reported reconfigurable antennas,[15] water acts as a dielectric resonator and they require large volume of water, which is inversely proportional to the operating frequency. As a result, the antennas become bulky, heavy weight, and unsuitable for applications that require antenna repositioning, like finding the direction of signal arrival or radar applications. By controlling liquid flow, water-air interface[16,17] is recently used to attain tunable properties. However, the physical structures of these water based devices are needed to be varied for reconfigurable operation, and this variation requires complex mechanical structures. Nonetheless, these methods are susceptible to vibration and not suitable for non-static and in-motion/vehicular applications.

In this work, we present a concept of frequency reconfiguration of liquid water-substrate antennas by using temperature as the controlling operator. The technique utilizes the temperature dependent dielectric properties of pure water. Tuning is achieved by designing the antenna to operate at different frequencies in different temperatures. While this reconfiguring technique takes advantage of high dielectric loading of water-based antennas, it has the following three main advantages over typical physically reconfigurable water-substrate antenna technique[15] in terms of real-world applicability: (i) the proposed technique does not require any physical changes to the antenna for reconfiguration, (ii) antennas are light weight, and (iii) as the antenna structure is fixed, the designed antennas are not motion sensitive. Thus, this technique is suitable for vehicular/maritime applications and is most effective and efficient in VHF and UHF bands.

Water demonstrates dispersive electromagnetic properties in different frequencies. Moreover, those properties significantly vary at different temperatures.[18] Although recently performance of temperature variable water based device is reported,[19] the applicability is only limited for electromagnetic absorption. However, in order to develop a frequency reconfigurable water-substrate based antenna on temperature control approach, the choice of frequencies is vital for radiation of electromagnetic waves with high efficiency. It is noted [Figs. 1(a) and 1(b)] that at low frequencies, 0 °C temperature water demonstrates highest permittivity $\varepsilon_r(f,T)$ and loss-tangent $\tan\delta(f,T)$ values. However, there is a resonance in $\varepsilon_r(f,T)$ plot, beyond which a steep downward trend in permittivity values is observed. The resonance shifts to

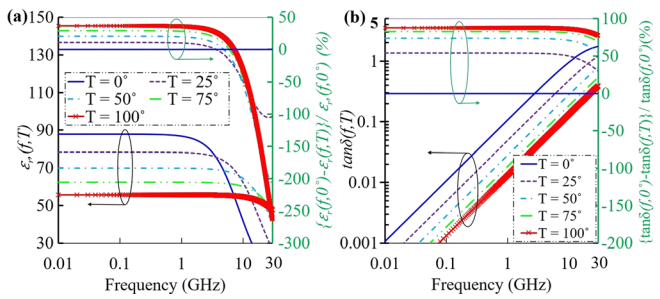

FIG. 1. Temperature dependence of the permittivity and loss tangent of water from 0.01–30 GHz: actual values of (a) relative permittivity [$\varepsilon_r(f,T)$] and (b) loss tangent [$\tan\delta(f,T)=\varepsilon_i(f,T)/\varepsilon_r(f,T)$] of water from 0 to 100 °C in 25 °C interval versus frequency, attained from the formulated equations for the complex relative permittivity, $\varepsilon^*(f,T)$ [$=\varepsilon_r(f,T)-j\,\varepsilon_i(f,T)$] of water.[18] The secondary axis represents the relative fractional variation of permittivity and loss tangent of water as the temperature changes from 0 °C to higher over different frequencies.

[a]Electronic mail: a.mobashsher@uq.edu.au

higher frequencies with the increase of temperature. In low frequencies, the permittivity changes monotonously with the increase of temperature from 0 °C and variation reaches as high as 32 (relatively around 36%) at 100 °C. On the other hand, the loss tangent varies non-monotonously. The rates of loss tangent enhancement for temperature increment are higher in the low temperature region and it becomes highest at 100 °C with relative variation of around 87% from those of 0 °C water.

Previously, vanadium dioxide (VO_2) is applied to develop thermally control hybrid-metamaterial.[17] But due to its high tan $\delta(f,T)$ values, VO_2 suffers from low transmission capability. Owing to the facts that (i) the antenna loading and miniaturization mostly depends on the effective permittivity, and (ii) loss tangent defines the material loss of the antenna,[20] both dielectric properties are critical for efficient antenna operation. Thus, high relative variations of permittivity provide the antenna an extended tunability and high loss tangent values result in low efficiencies. Following this criteria, it is noted that at high microwave frequencies (>10 GHz), the relative permittivity change can reach as high as 250% for 100 °C temperature variation, while the relative variation in loss tangent slightly changes; the designed antennas will provide the highest tunability. However, the antennas designed in this high microwave frequency region will also have very low efficiency due to the high tan $\delta(f,T)$ values. Although the efficiency can be improved by using partial loading technique,[15] it is unable to take full advantage of dielectric loading and thus reduces the tunable region. Hence, considering the actual values of loss tangent and relative changes of permittivity, it can be concluded that the temperature dependent reconfigurability by using water as a substrate is more appropriate for VHF and UHF bands.

In order to demonstrate omnidirectional radiation from a reconfigurable source, a water loaded dipole antenna having two thin copper strips is designed utilizing 3D electromagnetic simulation software CST Microwave Studio.[21] While other different types of omnidirectional antenna can be designed following the water loading technique, dipole type is chosen for simplicity and well-defined characteristics for comparison. The antenna [Figs. 2(a) and 2(b)] consists of two strips with total length of l_a and strip width of t_a, which are excited at the centre with a feeding gap of S. The metallic strips are positioned at the center of the water substrate, which has width, length, and height of t_w, l_w, and h_w, respectively. In order to emulate the realistic scenario, frequency dispersive complex relative permittivity [$\varepsilon^*(f,T)$] is defined during the simulation process.[21] The frequency dispersive effective permittivity due to the water loading of different temperatures on the dipole can be calculated using the following formula,

$$\varepsilon_{eff}(f,T) \approx 1 + (\varepsilon_r(f,T) - 1)\frac{(K_1 + K_2)}{2(K_3 + K_4)}, \qquad (1)$$

where $K_i = \frac{K(k_i)}{K'(k_i)}$, i = 1 to 3 and $k_1 = \frac{\sinh\left[\frac{\pi(l_a - S)}{2h}\right]}{\sinh\left[\frac{\pi(l_a + S)}{2h}\right]}$, $k_2 = \frac{\tanh\left[\frac{\pi S}{2(t_w + t_a)}\right]}{\sinh\left[\frac{\pi(S + 2l_a)}{2(t_w + t_a)}\right]}$, $k_3 = \frac{l_a - S}{l_a + S}$, $k_4 = \frac{S}{S + 2l_a}$. Equation (1) is calculated by transforming the total capacitance caused by the driven copper strips into equivalent parallel-plate capacitance using conformal mapping technique.[22]

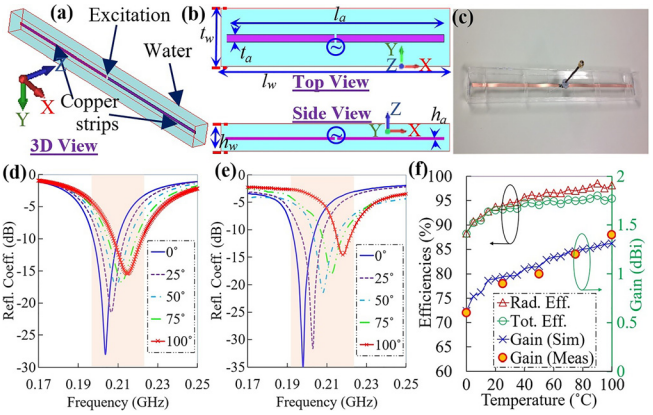

FIG. 2. (a) Perspective view of the designed antenna indicating different parts of it. (b) Top and side views illustrating the geometrical schematics of the water-substrate based antenna. (c) Photograph of the prototyped antenna. The (d) simulated and (e) measured reflection coefficient versus frequency performance of the optimized antenna. (f) The calculated radiation and total efficiencies of the reconfigurable antenna along with the simulated and measured gain values at resonating frequencies while operating in different temperatures.

Different parameters of the loaded dipole are optimized to attain wide tuning bandwidth and high efficiency. The optimization process includes a target function in terms of maximum bandwidth and efficiency, while the physical dimensions, as indicated in Fig. 2(b), of the water-loaded antenna are optimized to resonate in dipole mode. The antenna is prototyped [Fig. 2(c)] and measured for validation using a vector network analyzer (Rohde & Schwarz ZVA24). The water is contained in a transparent Plexiglas box with wall thickness of 1 mm. Owing to the thin layer of Plexiglass and its low permittivity (3.2), the box has negligible effect on the performance of the antenna. Nonetheless, the effect is considered in simulations and measurements. The reflection coefficient versus frequency graphs [Figs. 2(d) and 2(e)] show that the simulated water-based antenna demonstrates a frequency reconfigurable operation of around 14% bandwidth covering from 0.195 to 0.224 GHz frequency band using 100 °C temperature control. Because of the highest permittivity values at 0 °C, the antenna covers the lower end of the tunable bandwidth and the operating frequencies gradually moves to higher values with the increase of temperature and the reduction of permittivity. The prototyped antenna operates from 0.192 to 0.223 GHz, which is equivalent to 14.9% fractional bandwidth. The radiation efficiency of the antenna is also calculated from the 3D simulations of CST environment by taking both conductor and substrate material losses into account. Figure 2(f) shows that the antenna operates with more than 88% radiation efficiency over the reconfigurable region from 0 to 100 °C. Moreover, the total efficiency of the antenna, which considers radiation efficiency with the mismatch loss,[20] demonstrates more than 87% efficiency over the whole tunable range. The far-field radiation characteristics of the antenna is also measured in the standard anechoic chamber facility of the University of Queensland. The prototyped antenna attains highest gain of 1.4 dBi at 100 °C, while the gain is 0.6 dBi when operating at 0 °C temperature. The efficiency and gain increase systematically, however their variations can be related to the relative change

of the loss tangent, which is seen to change at slightly reduced rate in the higher temperatures when compared to the lower temperature end. Another reason for such reduced gain performance compared to the gain of a typical half-wave dipole in free space can be attributed to the reduction of equivalent electrical length[20] of the antenna due to the water-substrate loading. The size of the proposed antenna is around half of a typical half-wave dipole in free space. Since size of the antenna is one of the main limiting factors in VHF and UHF bands, such low-cost water-substrate loading can be used as an alternate to the typical varactor diode mounting, which results in low radiation efficiency and constrains the power handling capability of the antenna.[23] Nonetheless, the radiation patterns of the proposed antenna at the resonating frequencies for different temperatures are found to be of a typical dipole mode. No pattern deformation is noted for the loading of high dielectric water substrate.

From Fig. 3(a), it can be seen that the height (h_w) of water substrate has a dramatic effect on the resonance frequency and tunable band of the reconfigurable antenna. With the increase of vertical height of the substrate, the effective permittivity rapidly increases, which consequently reduces the resonating frequencies of the antenna. However, it is noted that as h_w gradually increases, the bandwidth (BW) of the antenna at individual temperatures decreases, resulting a gradual increase of quality factor (Q), following the relation,[24] $Q \approx 2/BW$. The Q factor of the antenna is defined[24] as the quotient between the stored and dissipated powers in the reactive field by

$$Q = \frac{4\pi f \, max\{W_e, W_m\}}{P_d}, \tag{2}$$

where W_e and W_m are stored electric and magnetic powers, P_d is the dissipated power and f is the frequency under

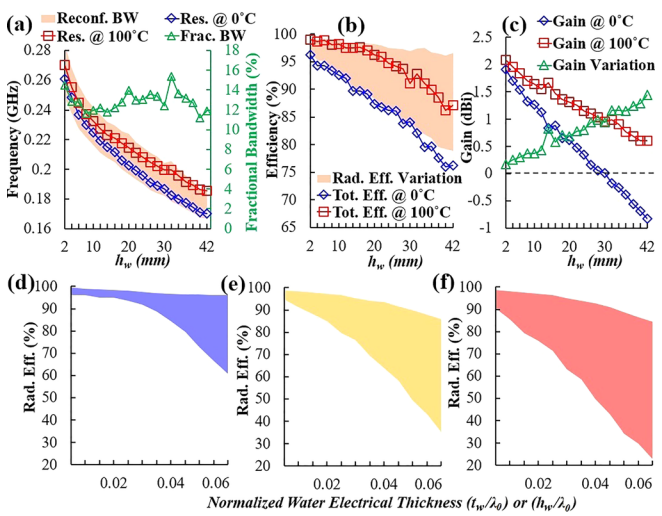

FIG. 3. Performance analyses of the temperature controlled reconfigurable antenna in terms of (a) operating frequency, (b) efficiency, and (c) gain, while the height of the water loading is varied with temperature change from 0 to 100 °C. The optimum parameters of the prototyped antenna are (in mm): t_a=5, t_w=40, l_a=380, l_w=400, h_a=0.2, h_w=20, and S=3. Radiation efficiency limits of a water-loaded dipole antenna as a function of normalized water electrical thickness (t_w/λ_0 or h_w/λ_0) at (d) 0.2, (e) 0.8, and (f) 1.5 GHz. The lower and upper ends of the shaded region denote efficiencies at 0 and 100 °C, respectively.

consideration. Noting the resonating frequencies decrease with the increment of h_w, an explanation can be drawn for such increment of Q. Owing to the fact that the effective permittivity values increase [$\varepsilon_{eff}(f,T)$ from Eq. (1)] with increasing h_w, the stored energies rapidly develop. The increase of stored energies is also evident from the increase of capacitive portion of the antenna impedance. Equation (2) suggests that as a result, the Q factor increases and consequently results in a reduction of the operating bandwidth at a specific temperature. Thus, the antenna becomes more sensitive to the parametric variations. Because of this increased sensitivity, the tunable bandwidth for temperature change between 0 and 100 °C remains around 13%, even though the gap between highest (at 100 °C) and lowest (at 0 °C) values of the resonances gradually extends. The lower end [Fig. 3(b)] of the radiation efficiency range is defined by tan $\delta(f,T)$ of 0 °C water. As the total amount of lossy water increases with increasing h_w, the radiation efficiency of the antenna decreases. However, the rate of radiation efficiency reduction at 100 °C is much slower when compared to that of 0 °C water-substrate antenna because of the much lower material losses in high temperatures. Similar conclusions of radiation efficiency can be drawn from Fig. 3(c) for the rate of peak gain (G) reduction.[24] However, when compared to the effect of h_w, the substrate loading effect of t_w is much less. Thus, in typical optimization process, we suggest emphasizing on h_w over t_w to accomplish compact reconfigurable antenna solution.

The bounds of radiation efficiencies of the water-substrate based antennas in different operating frequencies directly depend on the amount of substrate loading. As presented in the simulation derived results of Figs. 3(d)–3(f), the pattern of radiation efficiency variation of the antenna at a particular frequency is the same for both height (h_w) or thickness (t_w) variation. This indicates that the volume of the water substrate is the dominant factor along with the frequency-dispersive loss tangent of water in determining the efficiency. As noted from the radiation efficiency limits of Figs. 3(d)–3(f), while the proposed antenna is most efficient in VHF owing to low dielectric losses of water, high efficiencies can still be attained in high UHF (e.g., 1.5 GHz) with moderate water loading. However, the magnitude of compactness, which is proportional to substrate loading, reduces in this case. High temperature water is more suitable for efficient antenna reconfigurability. At 100 °C, water-based dipole antennas can provide more than 85% radiation efficiencies in high UHF region.

Temperature controllability of water-substrate based antenna can also be employed to develop directional reconfigurable antennas. To that end, a quasi-Yagi type[25] directional antenna is designed [Fig. 4(a)] by utilizing the previously described omnidirectional dipole and a reflector. The temperatures of both driven dipole and reflector are varied simultaneously from 0 to 100 °C. The extracted 3D full wave electromagnetic simulation results [Fig. 4(b)] show that the tunable antenna operates from 0.2 to 0.226 GHz, which is equal to 12.2% fractional bandwidth with the center frequency of 0.213 GHz. Measured impedance matching results are found to closely match the simulated performance. More importantly, the antenna demonstrates stable

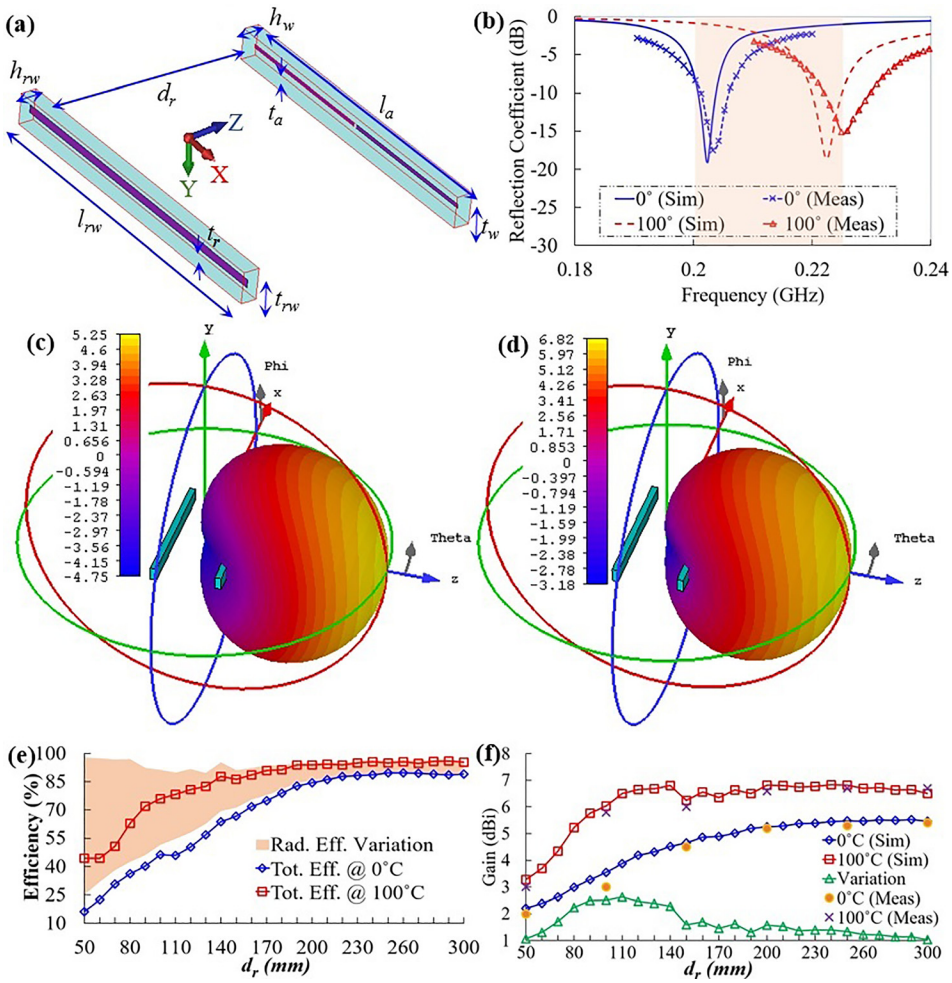

FIG. 4. (a) Schematic diagram of the water-loaded temperature controlled reconfigurable quasi-Yagi antenna. (b) Simulated and measured impedance matching characteristics of the directional antenna at 0 and 100 °C. The shaded region indicates the tunable region. The simulated 3D radiation patterns with respect to the antenna when operating at (c) 0 and (d) 100 °C temperature. (e) Radiation and total efficiency, and (f) simulated and measured gain performance of the directional antenna with different director (d_r) distances.

directional radiation patterns [Figs. 4(c) and 4(d)] over the whole bandwidth while varying the temperature. At the tunable ends of 0 and 100 °C, the antenna, respectively attains around 5.3 and 6 dBi gain along desired +Z direction with around 88% and 86% radiation efficiency accordingly. No side lobe is observed, which indicates enhanced polarization purity from the directional antenna.

Operation of the directional antenna crucially depends on the distance of the director (d_r). The radiation efficiency of the antenna [Fig. 4(e)] at 100 °C only slightly varies with the change of d_r due to low loss tangent values. Since this temperature state is at high end of the reconfigurable band, which ensures resonating at smaller wavelengths, the antenna attains peak gain values rapidly with a much smaller d_r value, when compared to the state of 0 °C, which operates at longer wavelengths. For the higher mutual coupling for longer wavelengths as well as the higher lossy substrate loading at 0 °C, the director needs to be kept at around 0.13 λ_0 away from the driven element in order to get high radiation efficiencies. It is noted that extending d_r beyond this distance does not add any additional performance advantage. The far-field gain performance of the antenna is verified through anechoic chamber measurements [Fig. 4(f)]. The optimum geometries of the antenna are (in *mm*): t_{rw}=40, l_{rw}=420, h_{rw}=20, t_r=10, and d_r=200.

While thermal tuning offers dynamic control of directional and omnidirectional antennas, its response time is inherently limited by the cooling timescale of water. Designing an adequate heating and cooling system can reduce the response, which can be calculated from the rate of heat transfer, Q by using the basic thermodynamics equation, $Q = MC\Delta T$, where the total mass of water, $M = 0.32$ and 0.65 kg accordingly for the omnidirectional and directional antennas, heat capacity of water, $C = 4.2\,\mathrm{kJ/(kg\,K)}$, and ΔT is the required temperature increment. In order to put this equation into context, around 6.1 and 12.4 s are required to increase the temperatures of the designed omnidirectional and directional antennas, respectively, by 10 °C using a typical 2.2 kW low-cost water-heater with small form factor. During the prototyped antenna measurement process, we utilized a standard water-heater. An infra-red thermometer (SainSonic DT8380) was used to ensure the operating temperature. A practical, low-cost way of implementing continuous temperature control of water is by mixing hot and cold water from different reservoirs. In this case, the inlet valve needs to be programmed to flow V_h and V_c volume of hot and cold water: $V_h = V_r\Delta T_h/\Delta T$ and $V_c = V_r\Delta T_c/\Delta T$, where V_r is the required volume of water, ΔT_h and ΔT_c are the temperature differences of the required temperature to those of hot and cold water, accordingly and ΔT is the temperature difference between hot and cold water. A thermostat can be utilized to maintain the feedback loop.

In conclusion, we have demonstrated the idea and prospects of reconfigurable water-substrate based antenna using temperature control technique. The antennas overcome the limitations of previously described physically reconfigurable

water-based antennas[15] and can be thus used as an alternative to the typical varactor diode based technique.[23] Two proof of concept antennas are designed. The performance of the antennas is explained in detail and suggestions for optimum tunable operation are also addressed. Despite the compact and light-weight (traditional water based antennas utilizes 6–10 l of water for reconfigurability,[15] while the proposed antenna use 0.32 and 0.65 l of water for omnidirectional and directional operation, respectively) construction of the proposed omnidirectional and directional antennas, the radiation performance, including efficiencies, gain, and radiation patterns, are comparable to previously described bulky water-based antennas.[15] Furthermore, compared to the frequency reconfiguration using the height control, the proposed tuning technique is less susceptible of vibration owing to its confined physical structure. This technique of reconfigurability is a strong candidate for non-static, low-cost solutions in VHF and UHF bands.

This work was supported by the University of Queensland Early Career Researcher Grant (Grant No. UQECR1719917).

[1]B. Gol, M. E. Kurdzinski, F. J. Tovar-Lopez, P. Petersen, A. Mitchell, and K. Khoshmanesh, Appl. Phys. Lett. **108**, 164101 (2016).
[2]R. C. Gough, J. H. Dang, M. R. Moorefield, G. B. Zhang, L. H. Hihara, W. A. Shiroma, and A. T. Ohta, ACS Appl. Mater. Interfaces **8**, 6 (2016).
[3]W. Zhu, Q. Song, L. Yan, W. Zhang, P.-C. Wu, L. K. Chin, H. Cai, D. P. Tsai, Z. X. Shen, T. W. Deng, S. K. Ting, Y. Gu, G. Q. Lo, D. L. Kwong, Z. C. Yang, R. Huang, A.-Q. Liu, and N. Zheludev, Adv. Mater. **27**, 4739 (2015).
[4]T. S. Kasirga, Y. N. Ertas, and M. Bayindir, Appl. Phys. Lett. **95**, 214102 (2009).
[5]T. Liu, P. Sen, and C. J. Kim, J. Microelectromech. Sys. **21**, 443 (2012).
[6]B. L. Cumby, G. J. Hayes, M. D. Dickey, R. S. Justice, C. E. Tabor, and J. C. Heikenfeld, Appl. Phys. Lett. **101**, 174102 (2012).
[7]M. R. Khan, G. J. Hayes, J.-H. So, G. Lazzi, and M. D. Dickey, Appl. Phys. Lett. **99**, 013501 (2011).
[8]M. Wang, C. Trlica, M. R. Khan, M. D. Dickey, and J. J. Adams, J. Appl. Phys. **117**, 194901 (2015).
[9]C. B. Eaker and M. D. Dickey, Appl. Phys. Rev. **3**, 031103 (2016).
[10]F. Zhang, Q. Zhao, L. Kang, D. P. Gaillot, X. Zhao, J. Zhou, and D. Lippens, Appl. Phys. Lett. **92**, 193104 (2008); D. Shrekenhamer, W.-C. Chen, and W. J. Padilla, Phys. Rev. Lett. **110**, 177403 (2013).
[11]F. Zhang, S. Feng, K. Qiu, Z. Liu, Y. Fan, W. Zhang, Q. Zhao, and J. Zhou, Appl. Phys. Lett. **106**, 091907 (2015).
[12]R. Peng, Z. Xiao, Q. Zhao, F. Zhang, Y. Meng, B. Li, J. Zhou, Y. Fan, P. Zhang, N.-H. Shen, T. Koschny, and C. M. Soukoulis, Phys. Rev. **7**, 011033 (2017).
[13]Y. Shi and S. Fan, Appl. Phys. Lett. **108**, 021110 (2016); J. Y. Kim, H. Kim, B. H. Kim, T. Chang, J. Lim, H. M. Jin, J. H. Mun, Y. J. Choi, K. Chung, J. Shin, S. Fan, and S. O. Kim, Nat. Commun. **7**, 12911 (2016).
[14]L. Lai, Y. Wu, P. Sheng, and Z.-Q. Zhang, Nat. Mater. **10**, 620 (2011); M. Liu, K. Fan, W. Padilla, D. A. Powell, X. Zhang, and I. V. Shadrivov, Adv. Mater. **28**, 1553 (2016).
[15]M. Zou, Z. Shen, and J. Pan, Appl. Phys. Lett. **108**, 014102 (2016); C. Hua and Z. Shen, IEEE Trans. Antennas Propag. **63**, 5185 (2015).
[16]N. Francois, H. Xia, H. Punzmann, P. W. Fontana, and M. Shats, Nat. Commun. **8**, 14325 (2017).
[17]T. Driscoll, S. Palit, M. M. Qazilbash, M. Brehm, F. Keilmann, B.-G. Chae, S.-J. Yun, H.-T. Kim, S. Y. Cho, N. Marie Jokerst, D. R. Smith, and D. N. Basov, Appl. Phys. Lett. **93**, 024101 (2008).
[18]W. J. Ellison, J. Phys. Chem. Ref. Data. **36**, 1 (2007).
[19]Y. Pang, J. Wang, Q. Cheng, S. Xia, X. Y. Zhou, Z. Xu, T. J. Cui, and S. Qu, Appl. Phys. Lett. **110**, 104103 (2017).
[20]C. A. Balanis, *Antenna Theory: Analysis and Design* (Wiley, New York, 2016).
[21]See http://www.cst.com/Content/Products/MWS/Overview.aspx for CST Microwave Studio®; A. T. Mobashsher and A. M. Abbosh, Sci. Rep. **6**, 37620 (2016).
[22]A. Abbosh, IEEE Trans. Antennas Propag. **61**, 2297–2300 (2013); R. Garg, I. Bahl, and M. Bozzi, *Microstrip Lines and Slotlines* (Artech house, London 2013).
[23]D. J. Gregoire, C. R. White, and J. S. Colburn, IEEE Antennas Propag. Mag. **54**, 251 (2012); M. S. Alam and A. M. Abbosh, IEEE Antennas Wireless Propag. Lett. **16**, 24 (2017); L. Liu, J. Rigelsford, and R. Langley, IEEE Trans. Antennas Propag. **61**, 3790 (2013).
[24]A. D. Yaghjian and S. R. Best, IEEE Trans. Antennas Propag. **53**, 1298 (2005); M. Gustafsson, D. Tayli, C. Ehrenborg, M. Cismasu, and S. Nordebo, FERMAT **15**, 1 (2016).
[25]A. Roederer, *IEEE Standard for Definitions of Terms for Antennas* (IEEE, New York, 2014).